FINAL CONTRACT REPORT

PLATE AND TUBE BRIDGE DECK EVALUATION IN THE DECK TEST BED OF THE TROUTVILLE, VIRGINIA, WEIGH STATION

Thomas E. Cousins, Ph.D.
Associate Professor
Department of Civil and Environmental Engineering

John J. Lesko, Ph.D.
Associate Professor
Department of Engineering Science and Mechanics

Virginia Polytechnic Institute & State University

Project Manager
Jose P. Gomez, Ph.D., P.E., Virginia Transportation Research Council

Contract Research Sponsored by
Virginia Transportation Research Council

Virginia Transportation Research Council
(A Cooperative Organization Sponsored Jointly by the
Virginia Department of Transportation and
the University of Virginia)

Charlottesville, Virginia

March 2004
VTRC 04-CR12

NOTICE

The project that is the subject of this report was done under contract for the Virginia Department of Transportation, Virginia Transportation Research Council. The opinions and conclusions expressed or implied are those of the contractors, and, although they have been accepted as appropriate by the project monitors, they are not necessarily those of the Virginia Transportation Research Council or the Virginia Department of Transportation.

Each contract report is peer reviewed and accepted for publication by Research Council staff with expertise in related technical areas. Final editing and proofreading of the report are performed by the contractor.

ABSTRACT

This report addresses the laboratory and field performance of multi-cellular fiber-reinforced polymer (FRP) composite bridge deck systems. We focus specifically on FRP decks produced from adhesively bonded pultrusions where the core of the deck possesses a square geometry running transversely to traffic. In laboratory tests, two schemes of loading patches were designed: a steel patch dimensioned according to the American Association of State Highway and Transportation Officials (AASHTO) Bridge Design Specifications, and a simulated tire patch constructed from an actual truck tire reinforced with silicon rubber. The stiffness, strength, and failure characteristics of the cellular FRP decks were examined using both loading patches.

Our research shows that the effects of the stiffness and contact conditions of loading patches are significant. The simulated tire loading develops greater deflections given the same static load. The failure mode is localized and dominated by transverse bending failure of the composites under the simulated tire loading as compared to punching shear for the AASHTO recommended patch load. A field testing facility was designed and constructed in which FRP decks were installed, tested, and monitored to study the decks' in-service field performance. No significant loss of deck capacity was observed after field service. However, the long-term field monitoring and testing results showed that the unsupported edges (or free edges) are undesirable.

FINAL CONTRACT REPORT

PLATE AND TUBE BRIDGE DECK EVALUATION IN THE DECK TEST BED OF THE TROUTVILLE, VIRGINIA, WEIGH STATION

Thomas E. Cousins, Ph.D.
Associate Professor
Department of Civil and Environmental Engineering

John J. Lesko, Ph.D.
Associate Professor
Department of Engineering Science and Mechanics

Virginia Polytechnic Institute & State University

INTRODUCTION

In the past decade, fiber-reinforced polymer (FRP) composite bridge deck systems have been experimentally implemented in bridge structures. An FRP bridge deck in this discussion is defined as a structural element totally or partially made from FRP materials that transfers loads transversely to the bridge supports such as longitudinal girders, cross beams, and/or stringers that bear on abutments. Research for developing FRP decks began in the early 1980s in the U.S. when the Federal Highway Administration initiated research aiming to transfer FRP composite technology to design and construction of bridge decks.[1] The first FRP deck research projects conducted in the U.S. were limited to the development of conceptual designs. The preliminary work reported by Henry[2] and Plecnik and Azar[3] examined the performance of several glass fiber reinforced polymer bridge deck configurations using finite element analysis (FEA). The results from these researchers indicated that the design was always controlled by deflection rather than strength.

In 1996, the first FRP reinforced concrete bridge deck was built in West Virginia, and the first all-composite vehicular bridge deck was installed in Kansas.[4] Since that time, a number of papers and reports concerning research in FRP bridge deck development have been published.[5,6,7,8,9,10,11,12] Today, the development of FRP decks has expanded beyond academia. There are a number of companies developing and producing FRP decks. World wide, there are many completed or currently underway bridge projects that use FRP decks. Typically the costs of these systems far exceed those of a reinforced concrete deck; therefore the development of a more cost-effective FRP bridge deck system is warranted. This research examines the use of pultruded, off the shelf components as a lower cost alternative FRP bridge deck system.

PURPOSE AND SCOPE

In an attempt to address this need this project investigates the laboratory and field characterization/performance of a multi-cellular modular FRP bridge deck systems. Specifically we examine a deck produced from adhesively bonded pultrusions, where the pultrusions are from off the shelf components. The characterization methods cover both laboratory testing procedures and field test techniques. In laboratory testing, a simulated tire patch was designed to approximate realistic tire contact loading conditions. The behavior of the FRP decks under the simulated tire loading patch is compared with the behavior under a steel loading patch sized according to the AASHTO bridge design specifications.[13] The fatigue and service life performance of FRP decks was investigated by utilizing a testing facility in the entrance ramp of a weight station. Deflection and strain response of the FRP deck subjected to field service loading are presented. A deck panel was tested in the laboratory prior to field installation. After 8 months in service (about 4 million fatigue loading cycles produced from traveling trucks), the deck was removed and tested in the laboratory to failure to study residual stiffness and strength. Another FRP deck was installed in the field-testing facility and was monitored to investigate the performance of FRP decks under long-term in-service field conditions.

DESCRIPTION OF THE FRP BRIDGE DECK SYSTEM

Efforts have been made to develop multi-cellular modular FRP composite deck panels produced from off-the-shelf FRP pultruded components.[9] The FRP deck system is fabricated by adhesively bonding standard pultruded structural square tubes and plates produced by Strongwell Corp. of Bristol, Virginia.[14] The deck's FRP components consist of A-glass and E-glass mats and roving. These components are produced from E-glass roving and continuous strand mat with a polyester resin, including additives such as pigments, fire retardants, mold releases, and clay filler. Additional A-glass random mat is used as the outside layer of the shapes for corrosion resistance. The deck system under experimental investigation here utilizes 10 pultruded square tubes running transverse to the traffic direction to form an FRP tube assembly. The tubes are bonded using epoxy adhesive with a working time/pot life of 3 hours and a cure time of 8 hours given a standard mix ratio. Through-rods run transverse to the direction of the tubes, securing the tubes in a plane during curing. This assembly is then bonded with two skin plates (top and bottom) using epoxy adhesives to form an FRP bridge deck. The bonding of these pultrusions is accomplished through the use of a vacuum bagging technique that ensures uniform pressure of the plates on the tube assembly. Our experience shows that vacuum bagging is very effective at producing quality bonds between the plate and tube assembly.

The modular FRP deck system presents an opportunity to alter the design (i.e. change in plate thickness or tube size) to accommodate particular service environments without the expense of modifying tooling. The thickness, modulus and other properties of the top and bottom skin plates as well as the internal tube size can be customized to various applications with different design requirements. This modular FRP deck system allows bridge designers the ability to optimize the deck characteristics to efficiently address various service requirements. The evolution of this prototype FRP composite deck system began in 1996 with the development by the authors and Strongwell Corp. of a proposed 5 inch thick bridge deck system for the Schuyler Heim Bridge in California.[9] The original development involved finite element modeling and testing to optimize the deck design for that specific

application. Development continued with the awarding of the project described here in and expanded to developing a nominal 6 ¾ inch thick deck system for larger support girder spacings.[15,16,17]

After the characterization of the prototype FRP deck panel[9] incorporating 102x102x64mm (4 ft x 4 in. x ¼ in.) tubes, four additional decks were built and tested using 152 x 152 x 95mm (6 in. x 6 in. x 3/8 in.) tubes. These four decks are referred to by phases, namely Phases I through IV decks.[15,16,17] A summary of comparisons for Phase I to Phase IV decks is presented in Table 1. Not including wearing surface, the decks are 4.65 m (15¼ ft) long, 1.52 m (5 ft) wide, and 17.2cm (6¾ in.) thick. An overview of the FRP deck panel over three supporting steel I beam girders is shown in Figure 1. The Phase I deck was laboratory tested for stiffness under service load and then to failure. The Phase II deck was tested for stiffness before being placed in a field-testing bed (discussed later). Following 8 months of field service, this deck was laboratory tested for stiffness and then to failure. The results from Phase II deck test provided information on the durability of the deck. The Phase III deck was laboratory tested for stiffness under the design service load and then placed in the field-testing bed. The Phase III deck remained in service from July 2001 till November 2002. Stiffness tests were performed in the field to observe any changes that may have occurred due to truck traffic. The Phase IV deck was modified and designed based on results from an analytical analysis and served as a laboratory specimen to investigate design parameters, such as adhesives and bonding techniques and the number of transverse steel rods, have on the deck's stiffness and strength.[18,19]

This deck was tested in the laboratory for stiffness and then ultimate strength given various loading patch designs. Since this deck would not be used for field testing, no wearing course was applied to the top surface. In order to estimate the stiffness gained, if any, by the presence of the steel through-rods, the number of rods in the deck was varied. On one half of the deck (or West span), only one through-rod was included for mechanical fastening, where as on the opposing span

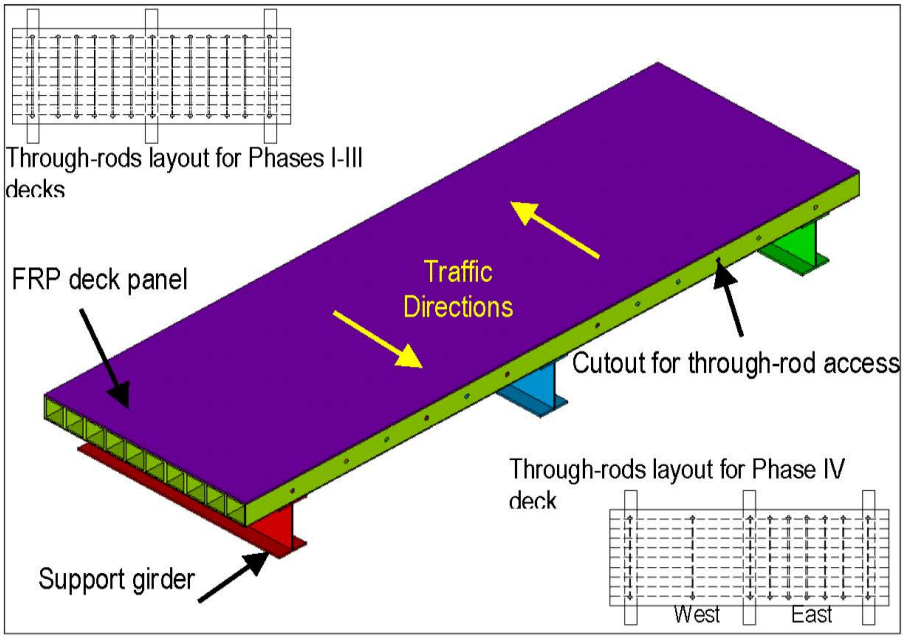

Figure 1 Overview of the investigated FRP bridge deck system

Table 1. Summary of comparisons for Phase I to Phase IV decks

		Phase I Deck	Phase II Deck	Phase III Deck	Phase IV Deck
Pultrusion of Square Tubes		Non-uniformity of tube-wall thickness due to variability of mandrel position inside the die	Higher quality control, tube-wall thickness much more uniform	Higher quality	Same as Phase III
Joining Adhesive		Shell 828 (epoxy)	Magnabond 56 (epoxy)	Same as Phase II	Same as Phase II
Number of Through-rods		12 Pultruded fiberglass	13 Cold drawn steel	Same as Phase II	9 Cold drawn steel rods (5 in east, 1 in west, 3 connection rods)
Plate Thickness (mm)		Top and Bottom: 9.5	Top and Bottom: 9.5	Top and Bottom: 9.5	Top: 12.7; Bottom: 6.35
Plate-to-tube Bonding Technique		50-pound weights placed on top of plates (one side of deck panel at a time)	Pates bonded to top and bottom surfaces of tubes; deck panel then vacuum bagged	Same as Phase II	Same as Phase II
Wearing Surface		Applied onto plates prior to plates being bonded to tubes	Applied after entire panel was vacuum bagged; Top surface sanded prior to application	Same as Phase II	No wearing surface
Loading Patch		Steel loading patch	Steel loading patch	Steel loading patch	Steel and tire[1] patches
Deck-to-Girder Connection		Through panel steel bolt with a sleeve [Figure 2(a)]	Steel bolt connecting deck bottom flange and support top flange [Figure 2(b)]	Steel Hook-bolt connecting through-rod and support's top flange [Figure 2(c)]	Same as Phase III
Deflection Index[2]	**Center**	L/398	L/426 [L/373[3]]	L/344	L/378[4]; L/218[5]
	Edge	L/247	L/268 [L/210[3]]	L/213	L/227[4]
Safety Factor[6]		4.12	5.08[6]	N.A.	4.50 (east); 5.27 (west)
Field Exposure		N.A.	8 months (4M cycles)	14 months (7M cycles)	N.A.
Failure Mode		Punching shear around the load plate [Figure 10a]	Punching shear at center and shearing at the edge [Figure 10b]	Cracking at unsupported edges under field loadings	Separation under bending (Fig.11), and cracking at cutouts (Fig.12)

(1) Simulated tire patch was used for failure test; (2) Deflection Index = (Span Length) / (Max. Deflection under Single Patch Loading at Deign Load) obtained from laboratory testing; (3) Post-field test after 8 months field service; (4) Under Steel Loading Patch; (5) Under Simulated Tire Patch; (6) Safety Factor = (Load at Failure) / (Design Load, 116kN); (6) After 8 months field service

(or East span), 5 evenly located transverse rods were spaced (the same as Phase I, I and III decks on this span), as seen from "through-rods layout for Phase IV deck" in Figure 1. This design was investigated to assess the effects of the number and location of transverse rods on the overall behavior of the deck system.

CONNECTION OF THE FRP BRIDGE DECK SYSTEM

Three deck-to-girder connection designs have been developed and investigated in these FRP deck panels. The Phase I deck was supported during testing by three W18×40 steel beams spaced 1.98 m (6.5 ft) apart to create two equal spans. The deck was fastened to the supports using a 12.7 mm (½ in.) diameter A325 bolt in twelve locations (four to each support beam). A section of the top plate and wearing surface was counter bored at each connection location. A hole was then drilled though the deck and at the corresponding location on the top flange of the support beam. The bolt placed thought the hole was to bear on a metal sleeve inside the deck tubes, shown in Figure 2 (a). A new deck-girder connection for the Phase II deck, shown in Figure 2 (b), included a 19mm (¾ in.) diameter, 57 mm (2¼ in.) long A325 steel bolts connecting the bottom flange of the deck system to the top flange of the support beam. Washers were used to prevent local bearing damage. The six connections were in the outermost two tubes to each support beam. This configuration was tested in both the laboratory and field and performed relatively well but was undesirable due to constructability issues (alignment and bolt access).

The support set-up for Phase III and Phase IV decks consisted of the deck spanning over three W14×48 support beams spaced at 1.98 m (6.5 ft.) center-to-center. The decks were connected to these support members at six points by way of the hook-bolt over through-rod connection shown in Figure 2(c). The detailed deck-to-girder connection using the J-hook bolt for the Phase III and Phase IV decks is shown in Figure 3. Connection points are shown as points marked by an "X" mark on a plan view of the deck in "Plan view of connection points" in Figure 3. The hook bolts used were fabricated from 19 mm (3/4 in.) diameter C-1018 steel rod. The rod was cut and then one end was bent 180° with a radius of approximately 12.7 mm (½ in.). The opposite end of the length of rod was threaded. The hooked bolts were placed over the 25 mm (1 in.) diameter through-rods through the slotted holes made in tubes two and nine during the fabrication of the deck. The deck was then lowered into place, aligning the bolts with 21mm (13/16 in.) diameter holes previously cut into the top flanges of the support members. The bolts were secured using two hex nuts, a flat washer, and a locking washer. This hook-bolt connection is approximated as a simply supported boundary condition of the deck panel, since there is only slight rotational restriction between the J-hoop and the transverse steel rod. The connections designs presented above are not intended to develop composite action between the deck and support girders.

TEST METHODS

To date, no specifications are in place for the design and testing of FRP bridge decks. The design loads and tire contact areas specified by the American Association of State Highway and Transportation Officials (AASHTO) Standard Specifications for Highway Bridges[20] and the AASHTO LRFD Specifications[13] are for reinforced concrete decks. In past studies of FRP decks, however, the AASHTO specifications have been used for lab testing without consideration of the differences between FRP decks and reinforced concrete decks.

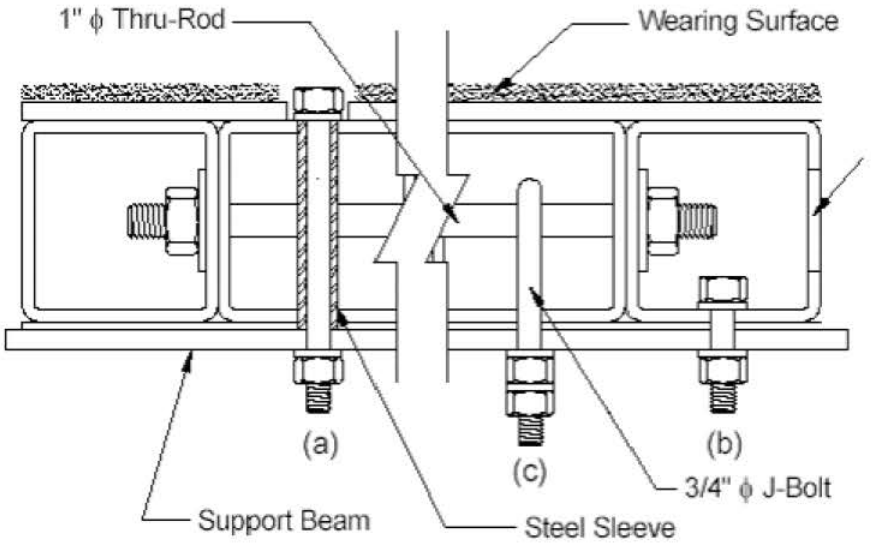

Figure 2 Connections for Decks Phase I (a), Phase II (b), and Phases III and IV (c).

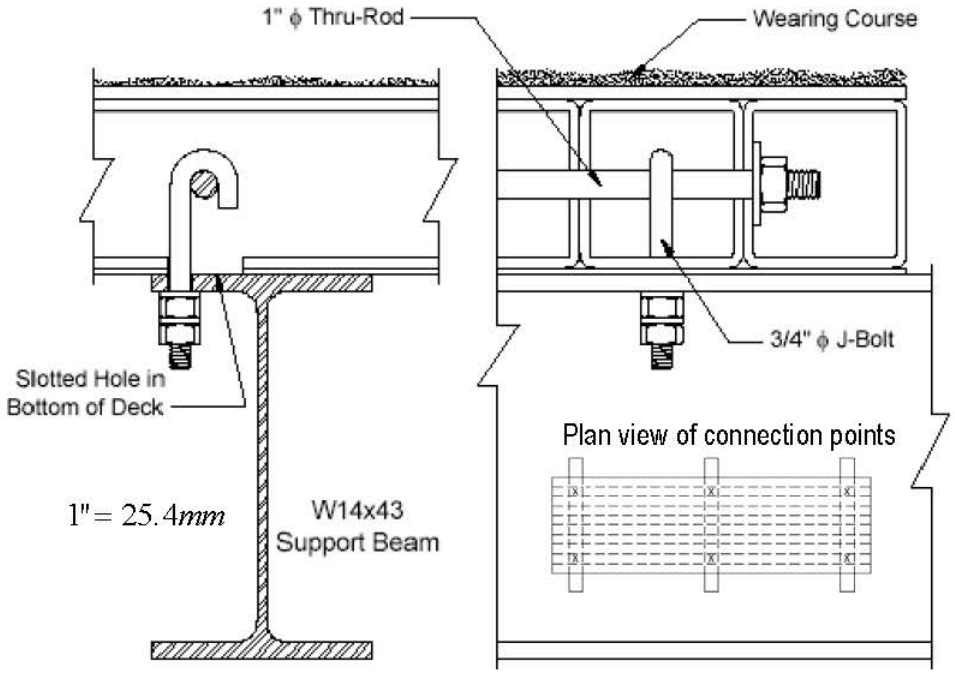

Figure 3 Deck-to-Girder connection details for Phase III and Phase IV decks

According to the AASHTO Standard Specifications,[20] when designing the superstructure members of a bridge, the specified loads are applied in critical locations to produce the maximum load effect. Bridge designers can apply the design wheel load over a finite surface area of the deck in computing the load effects on a bridge deck. This area is defined as the "tire contact area". The value of tire contact area can be obtained as: $A_c = k \cdot P$ where A_c is the tire contact area (in^2) and P is the wheel load (lbs), $k = 0.01$ (in^2/lbs). L is the Length of the contact area in the traffic direction, and W is the width. For a given design load, we have: $L = \sqrt{0.004 \cdot P}$ and $W = \sqrt{0.025 \cdot P}$ (L in *inch*, and P in *pound*); or $L \approx \sqrt{0.5806 \cdot P}$ and $W \approx \sqrt{3.6286 \cdot P}$ (L in *mm*, and P in *Newton*). AASHTO LRFD specifications[13] proposes a different method to obtain the tire contact area. According to this specification, the tire contact area of a wheel consisting of one or two tires shall be assumed to be a single rectangle (510 mm in width and 250 mm in length). It also points out that the above area and the specified load apply only to the design truck. The guideline for other truck loads (area in mm^2) may be calculated as: Tire Width $= P/142$ and Tire Length $= 165 \cdot Y \cdot (1 + IM/100)$, where Y is the load factor, IM is the dynamic load allowance percent, and P is the design wheel load in Newton. In this research, an HS25 design load with a 30% dynamic load allowance was used for stiffness testing. Therefore, the design load at each wheel in lab testing was 116kN (26 kips).

Although the above mentioned specifications are proposed for reinforced concrete bridge decks, many researchers have used this method to analyze and test FRP decks. The tire contacting area for our loading is calculated as 280 mm–508 mm (11 in.-20 in.) according to AASHTO LRFD specifications.[15] A stepped steel plate was made for lab testing according the above tire contacting area, which is shown in Figure 4 (a).

The results from 3-D finite element analysis for the whole bridge deck system revealed severe localized stress/strain concentrations at some critical locations (the edges of the steel loading plate and areas above the internal tubes' web.[19] Also, previous deck testing showed that a local punching shear failure occurred when loading through steel plates.[15] Given the relative local flexibility of the FRP composite cellular decks as compared to the steel plate, the nature of contact changes as a function of loading/deformation of the deck. Such local changes in compliance do not exist in concrete decks. Test results from the tire research community show that the normal stress distribution of a real truck tire is not uniform and more parabolic.[21] The above considerations led to the development of a simulated tire loading patch design. The simulated tire patch was constructed from a truck tire internally reinforced with silicon rubber (Figure 4(b)), and mimicked the contact loading conditions of an actual truck tire. A 23 cm (9 in.) wide truck tire was cut into quarter pieces. Then two pieces were filled with silicon rubber gel. After 24 hours of cure at room temperature, the rubber-reinforced-tires were ready for testing. The contact stress distributions for both patches were compared using pressure sensitive films. The footprints obtained from pressure film sensor are shown in Figure 5. The footprint of the simulated tire showed a similar pressure pattern as to that of an actual truck tire. The normal stress contour for the steel plate shows that stress concentrations occur at the patch edges.

A qualitative 2D loading patch (deck surface contacting analysis via finite element modeling[22]) showed that there were severe stress/strain concentrations at the contacting edge areas between the deck top plate and the steel plate, while no stress concentration was observed in the middle of contacting area (see Figure 6.a). For the simulated tire patch, it was observed that stress concentrations occurred at the central part of the contacting area. However, no concentration was observed at the contacting edges for

the simulated tire patch (Figure 6.b). These results will be compared to experimental results presented below.

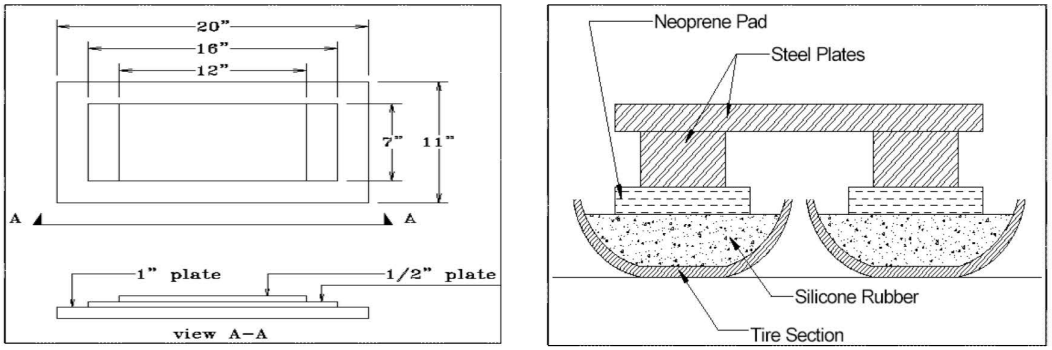

a). Steel Patch $(1" = 25.4mm)$ b.) Simulated Tire Patch (not to scale)

Figure 4 Loading patches used in laboratory tests

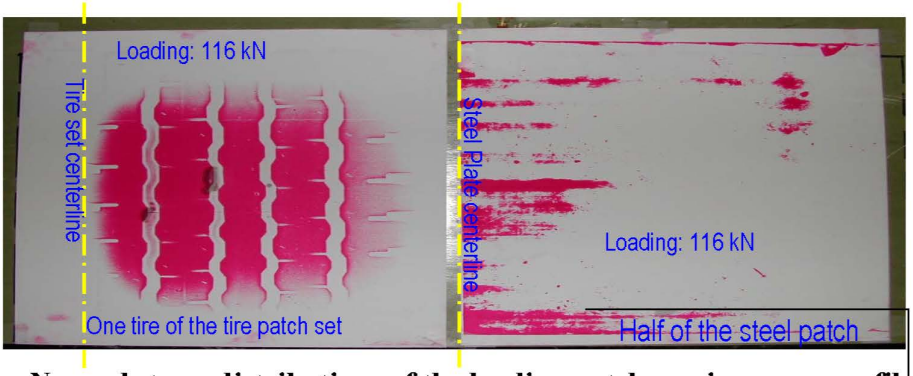

Figure 5 Normal stress distributions of the loading patches using pressure film sensor

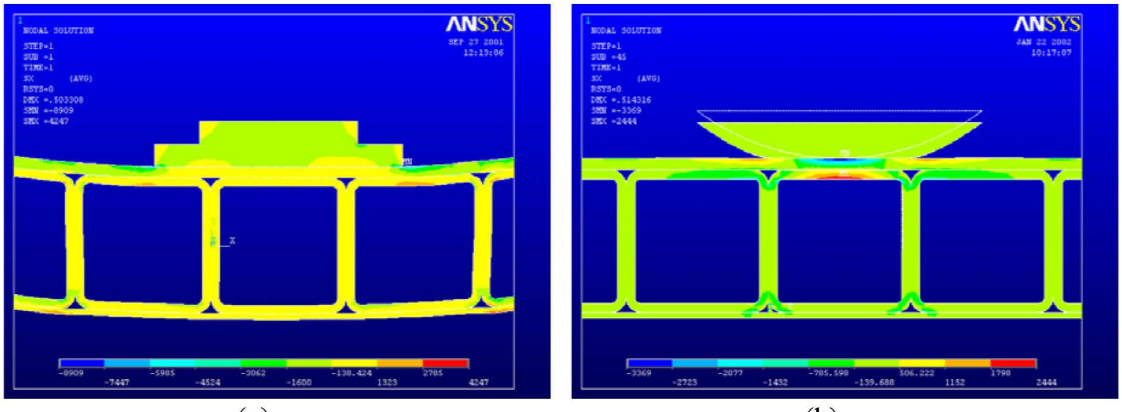

(a) (b)

Figure 6 Comparisons of transverse stress of the steel patch (a) and the tire patch (b) from finite element analysis

Laboratory Test Procedures

Similar test setups were used for all of the laboratory tests. Test loads were applied to each deck through loading patches by a hydraulic cylinder mounted on a load frame. The deck was transversely supported by three steel wide flange beams spaced 198 cm (78 in.) apart (see Figure 1). Loading locations were positioned as shown in Figure 7. Note that the transverse edges are unsupported to represent a worst case scenario.

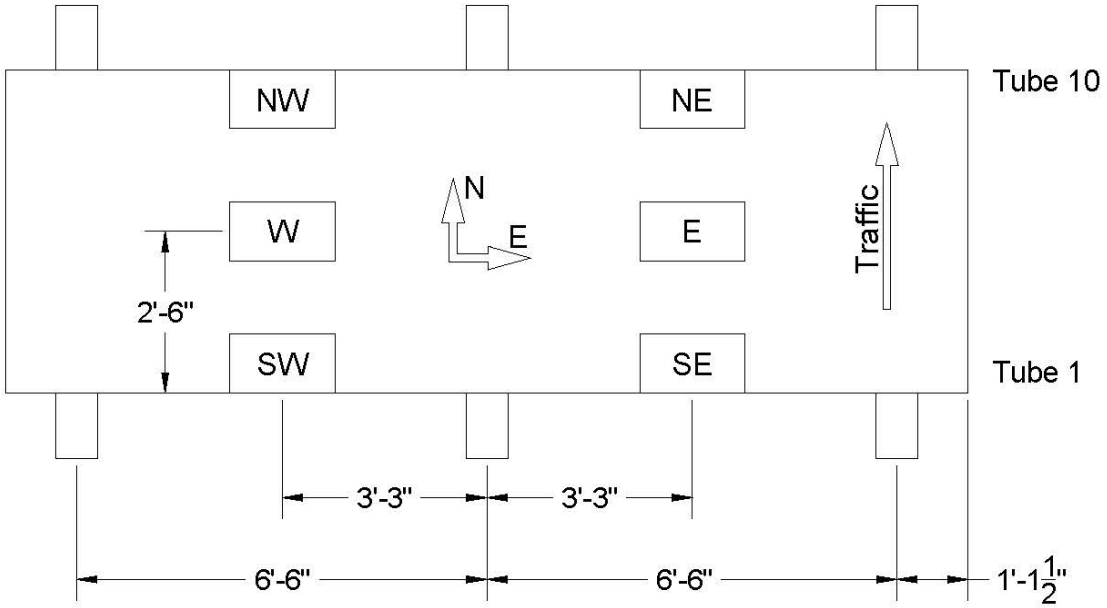

Figure 7 Locations of loading patches

The locations of loading patches as well as the determination of which patches would be loaded in each test were designed to simulate the support conditions on a real bridge (Figure 7). The transverse spacing of the girders was set to match what would be typical for this deck in a real bridge. Loading mode 2-5 (M2-5) will be used to simulate a truck axle load at the deck span centers. Loading modes 1-4 (M1-4) and 3-6 (M3-6) will be used to simulate an axle load at northwest & northeast and southwest & southeast regions, respectively. Modes 4-6 (M4-6) and 1-3 (M1-3) will be used as additional experimental reference data for results comparison from analytical work.[23] Mode 2 (M2) and mode 5 (M5) will be the loading locations for failure tests. Deflections were recorded at six locations, (NW–northwest, CW–central west, SW–southwest, NE–northeast, CE–central east, SE–southeast), as shown in Figure 7. Note that the NW (northwest) deflection was the vertical deflection of the bottom surface of the deck at the center of loading patch 1. The wheels of an AASHTO design truck are 183 cm (72 in.) apart; however, the East and West tire patches were spaced 198 cm (78 in.) apart to allow each tire patch to be placed in the middle of each span. With each tire patch positioned in the middle of each span, it was expected that the deck would experience higher strains (over the middle support) compared with tire patches spaced 183 cm (72 in.) apart. The orientations of the tire patches in the tests were selected to investigate the expected "worst-case" scenarios with respect to strains and deflections. Strain gages were placed along the middle of each span. Internal gages were placed during the fabrication process at the plant. These gages are placed on the tube corners/fillets prior to the application of the top and bottom plates. Strain gages were also mounted on the exterior of the top skin

plate to determine both longitudinal and transverse strain. On the bottom of the tubes, gages were mounted on the tube filets to mirror those on the top, as well as longitudinal and shear gages mounted in the center bottom of the third tube. Further details of the laboratory testing program are reported in theses by Temeles,[15] Coleman,[16] and Zhou.[17]

Field Test Procedures

To assess long-term performance and investigate the field performance characteristics of FRP deck systems, a facility was constructed to examine FRP bridge decks in service. This testing facility was put in place at the Troutville, Virginia weigh station (Interstate-81 North, Mile 148) in November of 1999. The facility was constructed on the entrance ramp of the northbound lane (see Figure 8). The weigh station site is a low risk setting where the traffic can be controlled to allow for deck modifications, inspection and controlled vehicle field testing. Steel access panels positioned at the approaches of the deck section allow for instrumentation and inspection of the deck. In the present configuration the edges of the deck are unsupported representing a worst case scenario. Over 200,000 trucks (over 100,000 on each side) pass through the Troutville weigh station each month.[14] A typical truck traveling through the testing facility produces five loading peaks. Therefore, there are about 0.5 million cycles of fatigue loading on the deck each month. Because of this high volume of traffic, the deck is subjected to a significant number of cycles of a high load. The deck panel is also exposed to realistic environmental conditions (varying temperature and moisture etc.) allowing researchers to investigate the long-term durability of the bridge deck panel.

Phase II and Phase III decks were implemented in the deck testing facility and fully described by Temeles[15] and Coleman.[16] The decks were supported by three steel wide flange beams setting on a concrete slab (see Figure 8). The steel beams support the FRP deck and two 4.57 m × 0.76 m (15 × 2.5 ft) steel access panels on each side of the deck. The detailed design and installation procedures of the testing bed are provided by Temeles.[15]

Figure 8 FRP deck field testing facility at the weight station

RESULTS

Effects of Through Rods on Deck Behavior

The effect of through rods on deck performance was evaluated because the installing of the through rods requires drilling through the square tubes. The cutouts in the tubes break reinforcing fibers and bring stress concentrations around the cutout regions. Studies from three dimensional finite element analysis showed that the contributions of the rods to the deck stiffness were insignificant, and a reduction of through rods in the deck would produce improved overall performance and reduce the cost of the deck.[19] To investigate the effects of through rods on the stiffness and strength, a deck (Phase IV deck) was designed and fabricated for laboratory testing. The experimental results for this study are presented in this section. The deflection-load and strain-load plots for M2 and M5 loading modes from laboratory tests are summarized in Figure 9(a) and Figure 9(b) with both the steel patch and the simulated tire patch.

These strains are all longitudinal strains (i.e. tube direction) from the gages on the bottom surface. For both loading patch conditions, the load-deflection curves and load-strain curves are linear for both spans. However, some nonlinear behavior was observed in the decks just prior to failure. Larger slopes of the load-deflection curves were observed for the steel tire patch. From the maximum deflections and curve slopes of Figure 9(a), it is evident that the west span (with 1 transverse rod) is stiffer than the east span (with 5 transverse rods). The maximum strains and the load-strain curve slopes also showed a similar trend. The west span (with 1 transverse rod) has less strain per unit load than the east span. It was expected that the east span with 5 rods would be stiffer than the west span; however, the experimental results show that the opposite occurred. In fact, the stiffness of the west span

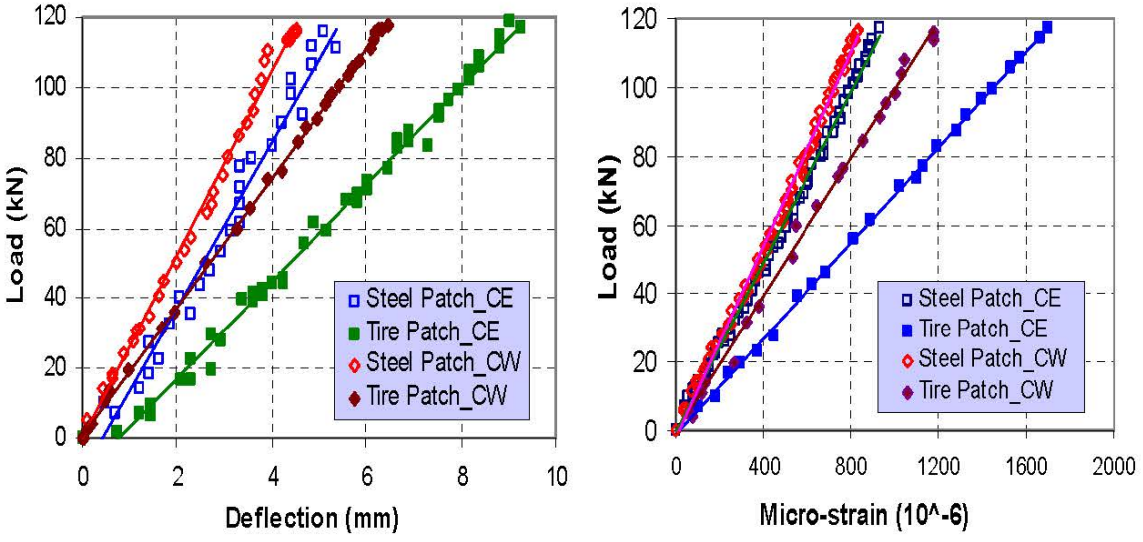

a) b)

Figure 9 Deflection-load curves (a) and strain-load curves (b) of Phase IV deck when loaded at central east (CE) and central west (CW)

measured as much as 40% more than that of the East span. This difference is attributed to the extra cutouts in the webs of the tubes (to allow the passing of the transverse rods) in the east span as compared to the west span; this may have contributed to the reduction in shear section allowing for greater deflection.

The maximum deflections and span-to-deflection ratios for different loading cases are summarized in Table 2 for a wheel load of 116 kN (26 kips) (HS25 wheel load including impact factor). The results in Table 2 show the effects of support conditions on the deck behavior: when the deck is loaded at the unsupported edges (M1-3, M1-4, M3-6 and M4-6) the corresponding maximum deflections are generally larger than the deflections loaded at the deck centers (M2, M5 and M2-5). In general, the west span (with one transverse rod) is stiffer than the east span (with 5 transverse rods). The recorded normalized maximum strain for each loading case is summarized in Table 3. It is seen from Table 3 that, under the same loading level, the maximum center span strains are generally smaller than the maximum strains at the free edges. However, all these maximum strains are much lower than the estimated components ultimate failure strains (0.8-0.15% for tubes and 1.1-1.6% for plates).[16] For other loading cases, it is also shown that the normalized maximum strain in the west span (with one transverse rod) is lower than the east span. After failure tests for both sides, the east span had an ultimate capacity of 520 kN (117 kips), while the west span had an ultimate capacity of 609 kN (137 kips). For both tests to failure linear behavior was observed up until failure other than some non-linear behavior immediately before failure. Clearly the additional though rods provided no significant increase in the stiffness or strength of the FRP deck system, in fact there is evidence that the opposite is the case.

Effect of Loading Patch Type on Deck Behavior

Three decks (Phases I, II and IV) were tested to failure. The failure test of Phase I deck (with wearing surface) was performed using steel patch after stiffness tests. The failure test of the Phase II deck (with wearing surface) was conducted using steel loading patches after being subjected to about 4 million loading cycles in the weigh station. The Phase IV deck was tested as received without wearing

Table 2. Summary for Maximum Deflection and Deflection-to-Span Ratio for Phase IV Deck

Loading Case		Maximum Normalized Deflection* (mm/kN)	Deflection/Span Ratio
M2 (West Span)	Steel	0.038	L/452
	Tire	0.054	L/317
M5 (East Span)	Steel	0.045	L/378
	Tire	0.078	L/218
M2-5 (Central)	West	0.033	L/519
	East	0.039	L/440
M1-3 (West Span)	North	0.071	L/241
	South	0.062	L/274
M1-4 (North Part)	West	0.058	L/293
	East	0.062	L/276
M3-6 (South Part)	West	0.058	L/293
	East	0.068	L/252
M4-6 (East Span)	North	0.067	L/256
	South	0.075	L/227

* Maximum Normalized Deflection= Maximum Deflection (mm)/Load (kN)

Table 3. Maximum Strain Comparisons for Phase IV Deck

Loading Locations	Maximum Normalized Strain ($\mu\varepsilon$ /kN)		Location of Maximum Normalized Strain
	Tensile	Compressive	
M2	8.85	-6.18	I_W / T_W
M5	9.27	-6.18	I_E / T_E
M2-5	8.40	-6.16	I_W / T_W
M1-3	14.98	-11.02	I_NW / T_SW
M1-4	12.91	-10.17	I_NW / T_SW
M3-6	12.26	-9.28	B_SW / T_SW
M4-6	15.47	-11.30	I_SE / T_SE

Maximum Normalized Strain = Maximum Strain ($\mu\varepsilon$)/Load (kN)

surface. The failure mode of the Phase II deck using steel loading patch is shown in Figure 10. Note that the failure mode of the Phase I deck was virtually identical to that of the Phase II deck. Detailed failure test data for the Phase II deck can be found in thesis of Temeles.[15] During failure testing, debonding (between the face sheets and tubes) was observed during the loading cycle at a load of about 245 kN (55 kips) for both decks. The Phase I deck failed at 476 kN (107 kips) for central span loading and consisted of a local punching shear failure (see Figure 10-a) directly under the steel patch edges. For the Phase II deck, one side was loaded at the center to failure and the other side loaded at the unsupported edge to failure. The failure mode of Phase II deck when loaded at the center was the same as Phase I deck (Figure 10.a) but with a larger ultimate capacity of 587 kN (132 kips). Shearing in the sidewall of the cell initiating from the underneath the loading patch (Figure 10-b) and controlled the failure of the other side of the Phase II deck when loaded at the unsupported edge, with the ultimate capacity of 378 kN (85 kips).

(a) (b)

Figure 10 Failure of Phase I Deck at the center (a) and Phase II Deck at the edge (b) using steel loading patch

As comparison, the failure of Phase IV deck using the simulated tire patch is shown in Figure 11. For both spans, debonding (between the face sheets and tubes) was observed when the load reached about 245 kN (55 kips). The east span failed at 520 kN (117 kips). For the west span (which has 1

through rod) the ultimate strength was recorded at 609 kN (137 kips). This is 17% higher than the east span (which has 5 through rods). Under the simulated tire loading conditions, no punching shear was observed. The deck components, top plate and the top flange of the tube, failed in bending with transverse separation as shown in Figure 11. The location of the central crack (see Figure 11) is at the center of the tube's top flange. The west span also failed as surface cracking (see Figure 11). For both spans, the failure areas were highly localized and under the center of the tire patch–deck contact area. The failure inside the tube assembly is shown in Figure 12 for Phase IV deck indicating tensile bending failure due to transverse or cross wise failure of the plate and tube. The shearing of the tube webs in east span (which has 5 through rods) was also observed (see Figure 12-a). The holes in the webs for the through bolts reduced the webs' resistance to bearing stress in the east span. However, no cracking was observed on the tube webs in the west span (Figure 12).

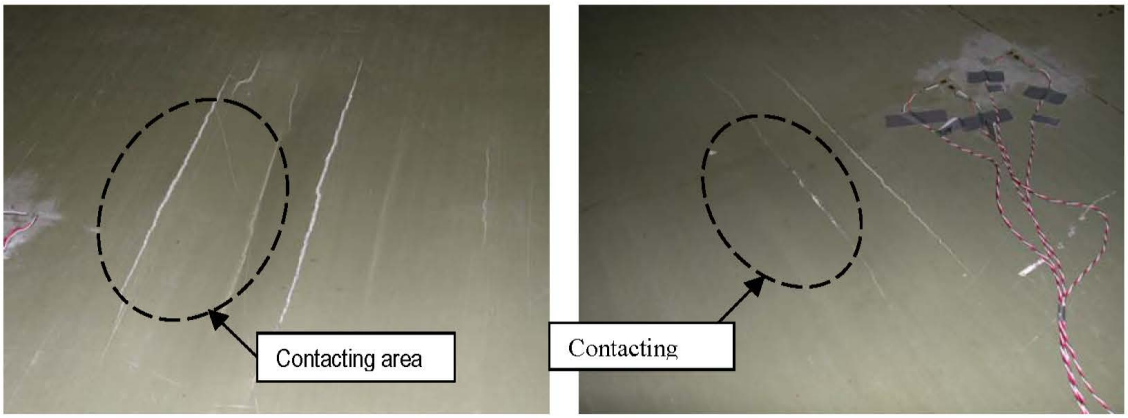

(a) Surface failure-east span (b) Surface failure-west span

Figure 11 Surface failure of Phase IV Deck using simulated tire patches

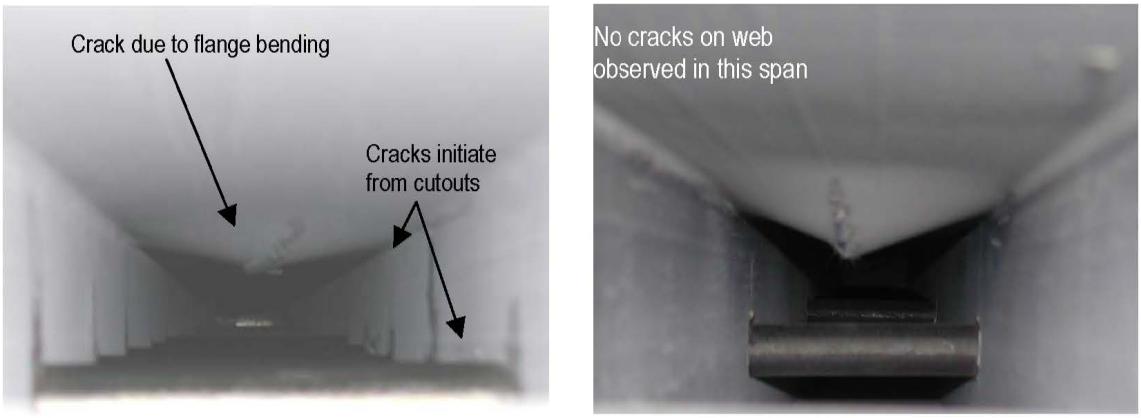

(a) Internal tube failure-east span (b) Internal tube failure-west span

Figure 12 Internal tube failure of Phase IV deck using simulated tire patches

The above test results provide important implications for cellular FRP deck design and testing: (1) The tire contact area and stress distribution over the contact area will affect the tested maximum

deflection, maximum strains, and the deck's ultimate capacity. (2) Under the same loading level, the free (or unsupported) edge maximum deflection and strains are generally larger than these when loaded at the span center. This indicates that failure is very likely at the free edges/unsupported edges and should be avoided in practice. The larger deflection and strains at the unsupported edges may also raise concerns related to the durability of the deck, i.e., the unsupported edges are weak regions. (3) Every effort should be made to reduce the number and size of cutouts in the web. The side of the deck with less through bolts was stiffer and stronger than the span that has more cutouts/ through-bolts.

Test Results from Decks Placed in Weigh Station

The Phase II deck was tested in the laboratory prior to field installation, and was removed and tested again in the laboratory after 8 months of field service (about 4 million cycles of truck loading). A comparison of pre-field and post-field normalized deflections (P/Δ (kN/mm)) and normalized strains (P/με (kN/1)) for the Phase II Deck are provided in Table 4. The table shows that the stiffness loss ranges from 12% to 25%, while the strength loss is small (the maximum loss is 7%). The stiffness loss is attributed to degradation of the deck materials due to exposure to the service environment at the weigh station. The failure load of the Phase II deck after 8 months field exposure was 587 kN (132 kips) when loaded at span center, which is higher than the failure load of Phase I deck [476 kN (107 kip) loaded at span center], and close to the Phase IV deck's failure loads 609 kN (137 kips) on the west span and 520 kN (117 kips) on the east span. The Phase II deck was tested with a steel plate load patch and had a failure mode similar to that of the Phase IV deck. Therefore, no ultimate capacity loss was observed for the Phase II deck after about 4 million cycles truck loadings.

Controlled vehicle field tests were performed at the test bed for Phase III deck on three different occasions spanning approximately one year to investigate the behavior of the deck under actual service loads and to monitor any loss in stiffness and strength during that time. Strains were recorded on all three dates (August 1, 2000, September 20, 2000, and September 27, 2001), and deflections were recorded on the second and third field tests. Since data from the August 2000 testing were incomplete, data from the September 2000 test and the September 2001 test will be compared to study the changes of stiffness and strength of the Phase III deck during the service period. Five axle orientations were used during the field tests with five runs performed at each orientation during testing.[16] A three-axle truck was driven at slow speed across the deck for each run. The distance from the front axle to the middle of the rear tandem axle was 4394mm (173 in.), and the distance between the two rear axles was 1346 mm (53 in.). The transverse distance between wheels was 2083 mm (82 in.). The tire contact areas are 228 x 241 mm (9 in. x 9.5 in.) for the front tires (two front tires) and 254 x 241mm (10 in. x 9.5 in.) for the rear tires (8 rear tires), where 241mm (9.5 in.) is the width of the tire contact area and is along the driving direction. The total weights of the truck were:[16] 234 kN (52.6 kips) on September 20, 2000, and 260 kN (58.5 kips) on September 27, 2001.

Due to loss of gages over time, it is not possible to compare all peak strains for each of the field tests. Field Test I refers to the field test conducted on September 20, 2000 (about 0.7 million cycles); and Field Test II refers to the test conducted on September 27, 2001 (about 7 million cycles). The deflection gages were all implemented on the bottom surface of the deck. The normalized deflection (P/Δ) and normalized strain (P/με) comparisons for several critical locations are provided in Table 5. Results from normalized deflection (P/Δ) showed that no significant stiffness loss was observed during these periods (up to about 7 million cycles). Stiffness gain was observed for several gages; however, the normalized strain (P/με) data showed the degradation of residual strength of deck components (12% to

19% reductions over the period). Later cracking of deck components was observed at the free edges, which indicates that free edges are vulnerable to dynamic mechanical and environmental fatigue loads.

Two types of connections were used in the Weigh Station to connect the Phase II and II deck panels to the supporting steel stringers (see Figure 2). For the Phase II deck the panel was attached using straight bolts installed through a whole in the sidewall of the external tube. The connection was undesirable due to constructability issues (alignment and bolt access). The Phase III deck was attached using a hooked-bolt around the steel through rods. This connection performed extremely well in the field and is a viable connection for future deck applications.

CONCLUSIONS AND RECOMMENDATIONS

The behavior of a multi-cellular FRP bridge deck system is investigated through laboratory tests and field tests. Four designs (called Phases I thought IV in this report) of a FRP deck system were used to develop an implementable bridge deck system. In laboratory tests, two different schemes of loading patches were developed: a steel patch sized according to the AASHTO bridge design specifications; and a tire patch made from a truck tire reinforced with silicon rubber. It was seen that, due to the localization of load, effects of the stiffness and contact conditions of loading patches are significant in the stiffness and strength testing of FRP decks. Because of its highly localized behavior, a simulated tire patch yielded larger maximum deflection and strain than the steel plate under the same loading level. The tire patch produced significantly different failure modes compared to the steel plate: a local bending mode with less damage under the tire patch; and a local punching-shear mode under the steel plate. The results from both laboratory and field tests indicate that the unsupported edges should be avoided in practice.

The behavior comparisons of the west span and east span of Phase IV deck indicate that the number of through rods in this FRP deck system can be significantly reduced and only need to be included to allow for the hooked bolt connection of the deck to supporting stringers. Comparisons for experimental results of the same deck (Phase II deck) from field tests and laboratory tests showed no significant strength and load-carrying capacity loss after 4 million cycles fatigue loading. Field monitoring of the Phase III FRP deck did not show significant stiffness loss from about 0.7 million loading cycles to about 7 million cycles of truck loading.

The FRP bridge deck system performed well in the intense service load environment of the Troutville Weigh Station. For example, the Phase II deck survived 4,000,000 truck loadings with some loss in stiffness (12 to 25%) and minimal loss in strength.

In summary the authors conclude the following: a) Due to the local effects of a real tire load, a simulated tire loading patch would be more appropriate in laboratory testing; b) The unsupported edges are vulnerable to deterioration under repeated loads; therefore, in practice, design and construction with free edges should be avoided; c) the hooked bolt connection should be used in future FRP deck applications; d) FRP decks made from adhesively bonded pultrusions are viable structures for highway bridge deck applications .

This project involved the development and implementation of a proposed FRP bridge deck system. The FRP deck developed was essentially a 5 foot by 15 foot panel. Four of these panels were

either tested in the laboratory and/or placed in the Troutville Weigh Station. As described above this research concentrated on specific aspects of FRP deck behavior but was not intended to develop a ready for market system. Further research is needed before this type of deck system is more than a special case option. The connection of adjacent panels was not investigated and this should be one focus of future research. Further investigation of environmental degradation is warranted. Also, design standards are not available and the FRP bridge deck industry has very few standards of performance or quality control developed.

REFERENCES

1. Zureick, A., Shih, B., and Munley, E. (1995), Fiber-Reinforced Polymeric Bridge Decks. *Structural Engineering Review*, 7(3), 257-266.

2. Henry, J.A. (1985), Deck Girders System for Highway Bridges Using Fiber Reinforced Plastics. M.S. Thesis, North Carolina State University, Raleigh, North Carolina.

3. Plecnik, J.M. and Azar, W.A. (1991), Structural Components in Highway Bridge Deck Applications. *International Encyclopedia of Composites* (Vol. 6), Lee, I. and Stuart, M., editors, VCH Publishers, New York: 430-445.

4. Market Development Alliance (2000), *Product Selection Guide: FRP Composite Products for Bridge Applications,* Busel, J.P. and Lockwood, J.D., editors, Harrison, New York.

5. Seible, F. (1996), Advanced Composites Materials for Bridges in the 21st Century. *Advanced Composite Materials Bridges and Structures*, Elbadry, M.M., editor, 17-40.

6. Lopez-Anido, R., GangaRao, H.V.S., Vedam, V., Overby, N. (1997), Design and Evaluation of a Modular FRP Bridge Deck. *Proceedings of the International Composites Expo '97*, 3 (E), 1-6.

7. GangaRao, H.V.S., Thippeswamy, H.K., Shekar, V., and Craigo, C. (1999), Development of Glass Fiber Reinforced Polymer Composite Bridge Deck. *SAMPE Journal*, 35(4), 12-24.

8. Salim, H.A., and Davalos, J.F. (1999), FRP Composite Short-Span Bridges: Analysis, Design and Testing. *Journal of Advanced Materials*, 31 (1), 18-16.

9. Hayes, M.D., Ohanehi, D., Lesko, J.J., Cousins, T.E., and Witcher D. (2000), Performance of Tube and Plate Fiberglass Composite Bridge Deck. *Journal of Composites for Construction*, 4(2), 48-55.

10. Karbhari, V.M., and Zhao, L. (2000), Use of Composites for 21st Century Civil Infrastructure. *Computer Methods in Applied Mechanics and Engineering*, 185, 433-454.

11. Qiao, P., Davalos, J.F., Brown, B. (2000), A Systematic Approach for Analysis and Design of Single-Span FRP Deck/Stringer Bridges. *Composites Part B: Engineering,* 31(6-7), 593-610.

12. Bakis, C.E., Bank, L.C., Brown, V.L., Cosenza, E., Davalos, J.F., Lesko, J.J., Machida, A., Rizkalla, S.H., and Triantafillou, T.C. (2002), Fiber-Reinforced Polymer Composites for Construction: State-of-the-Art Review, *Journal of Composites for Construction*, 6 (2): 73A-87.

13. American Association of State Highway and Transportation Officials (1998), *AASHTO LRFD Bridge Design Specifications (Second edition)*. Washington, D.C.

14. Strongwell Corp. (1998), *EXTREN Design Manual*, Strongwell Corp., Bristol, Virginia.

15. Temeles, A. B. (2001), Field and Laboratory Tests of a Proposed Bridge Deck Panel Fabricated from Pultruded Fiber-reinforced polymer Components. M.S. Thesis, Virginia Polytechnic Institute and State University, Blacksburg, Virginia.

16. Coleman, J. T. (2002), Continuation of Field and Laboratory Tests of a Proposed Bridge Deck Panel Fabricated from Pultruded Fiber-Reinforced Polymer Components. M.S. Thesis, Virginia Polytechnic Institute and State University, Blacksburg, Virginia.

17. Zhou, A. (2002b). Stiffness and Strength of Fiber Reinforced Polymer Composite Bridge Deck Systems. Ph.D. Dissertation, Virginia Polytechnic Institute and State University, Blacksburg, Virginia. (On-line at http://scholar.lib.vt.edu/theses/available/etd-10072002-164345/.)

18. Zhou, A., Lesko, J. J., Coleman, J. T., and Cousins, T. E. (2001a), Behavior of Multi-cellular Orthotropic FRP Composite Bridge Deck Under Static Loadings. *Proceedings of 16th Annual Technical Conference, American Society for Composites,* Blacksburg, Virginia (CD-ROM).

19. Zhou, A., Coleman, J. T., Lesko, J. J., and Cousins, T. E. (2001b), Structural Analysis of FRP Bridge Deck Systems from Adhesively Bonded Pultrusions. *Proceedings of the International Conference on FRP Composites in Civil Engineering, Hong Kong:* 1413-1420.

20. American Association of State Highway and Transportation Officials (1996), *Standard Specifications for Highway Bridges (16th Edition)*. Washington, D.C.

21. Pottinger, M.G. and McIntyre, J.E. (1999), Effect of Suspension Alignment and Modest Cornering on the Footprint Behavior of Performance Tires and Heavy Duty Radial Tires. *Tire Science and Technology,* 27 (3), 128-160.

22. Zhou, A., Lesko, J. J., Coleman, J. T., and Cousins, T. E. (2002a), Failure Modes and Failure Mechanisms of FRP Composite Bridge Decks. *Proceedings of the Third International Conference on Composites in Infrastructure*, San Francisco, California (CD-ROM).

23. Zhou, A., and Lesko, J. J. (2003), Structural Analysis and Behavior of Cellular Fiber Reinforced Polymer Composite Bridge Decks. Submitted to *Journal of Composite for Construction* (June 2003).